Chemistry & Biology
Article

Selective Overproduction of the Proteasome Inhibitor Salinosporamide A via Precursor Pathway Regulation

Anna Lechner,[1] Alessandra S. Eustáquio,[1,4] Tobias A.M. Gulder,[1,5] Mathias Hafner,[3] and Bradley S. Moore[1,2,*]
[1]Scripps Institution of Oceanography
[2]Skaggs School of Pharmacy and Pharmaceutical Sciences
University of California at San Diego, La Jolla, CA 92093-0204, USA
[3]Institute for Biomedical Technology, Heidelberg University and University of Applied Sciences, Mannheim 68163, Germany
[4]Present address: Natural Products Laboratory, World Wide Medicinal Chemistry, Pfizer Research and Development, Groton, CT 06340, USA
[5]Present address: Kekulé Institute for Organic Chemistry and Biochemistry, University of Bonn, Bonn 53121, Germany
*Correspondence: bsmoore@ucsd.edu
DOI 10.1016/j.chembiol.2011.10.014

SUMMARY

The chlorinated natural product salinosporamide A is a potent 20S proteasome inhibitor currently in clinical trials as an anticancer agent. To deepen our understanding of salinosporamide biosynthesis, we investigated the function of a LuxR-type pathway-specific regulatory gene, *salR2,* and observed a selective effect on the production of salinosporamide A over its less active aliphatic analogs. SalR2 specifically activates genes involved in the biosynthesis of the halogenated precursor chloroethylmalonyl-CoA, which is a dedicated precursor of salinosporamide A. Specifically, SalR2 activates transcription of two divergent operons—one of which contains the unique *S*-adenosyl-L-methionine-dependent chlorinase encoding gene *salL*. By applying this knowledge to rational engineering, we were able to selectively double salinosporamide A production. This study exemplifies the specialized regulation of a polyketide precursor pathway and its application to the selective overproduction of a specific natural product congener.

INTRODUCTION

The marine bacterium *Salinispora tropica* produces a series of potent natural product proteasome inhibitors, the salinosporamides, which are assembled by a hybrid polyketide synthase–nonribosomal peptide synthetase (PKS–NRPS) pathway from three distinct fragments (Gulder and Moore, 2010). Two of the biosynthetic building blocks, namely, acetate and the non-proteinogenic amino acid cyclohexenylalanine, are common to the natural salinosporamides. The third substrate, however, is derived from a mixture of branched malonate units that ultimately distinguishes between the different salinosporamide molecules. This difference in the chemical nature of the salinosporamide C-2 side chain has been shown to have a profound effect on their biological activity. The chlorinated salinosporamide A is not only the major family member produced in *S. tropica*, it is also its most potent. Structure-activity relationship studies (Macherla et al., 2005) together with high-resolution X-ray analysis of the inhibitor-proteasome complex (Groll et al., 2006) revealed that salinosporamide A's halogen acts as a leaving group upon proteasome β-subunit binding to heighten its potency as an irreversible inhibitor. Natural analogs without reactive C-2 residues are consequently reversible inhibitors of the 20S proteasome and are substantially less potent. Hence, salinosporamide A was selected and advanced to clinical trials as an anticancer agent, where it was produced for phase I studies by large-scale microbial fermentation (Fenical et al., 2009; Potts et al., 2011).

Biosynthetic studies illuminated the convergent pathways to the salinosporamides in which α-substituted malonyl-coenzyme A (-CoA) derivatives are individually synthesized and processed by the salinosporamide assembly line synthetase (Beer and Moore, 2007). An elaborate eight-step pathway converts *S*-adenosyl-L-methionine (SAM) into the dedicated salinosporamide A precursor chloroethylmalonyl-CoA (Eustáquio et al., 2009; Kale et al., 2010), and its encoding genes reside within the 41-kb *sal* gene cluster. The non-halogenated salinosporamides B, D, and E are conversely synthesized from ethyl-, methyl- and propylmalonyl-CoA (Liu et al., 2009), respectively, which with the exception of the latter are common primary metabolic precursors. Herein, we show that the biosynthesis of chloroethylmalonyl-CoA is differentially regulated by the pathway-specific regulator SalR2 and that its overexpression results in the selective overproduction of the clinically important salinosporamide A over its less active aliphatic analogs. This mechanism of regulation dedicated to precursor supply, which influences the production of a specific natural product over structurally related analogs, has to the best of our knowledge not before been described.

RESULTS

Identification of the Salinosporamide A-Specific Pathway Regulator SalR2

The *sal* biosynthetic gene locus contains three regulatory genes among its 31 open reading frames. Bioinformatics analyses

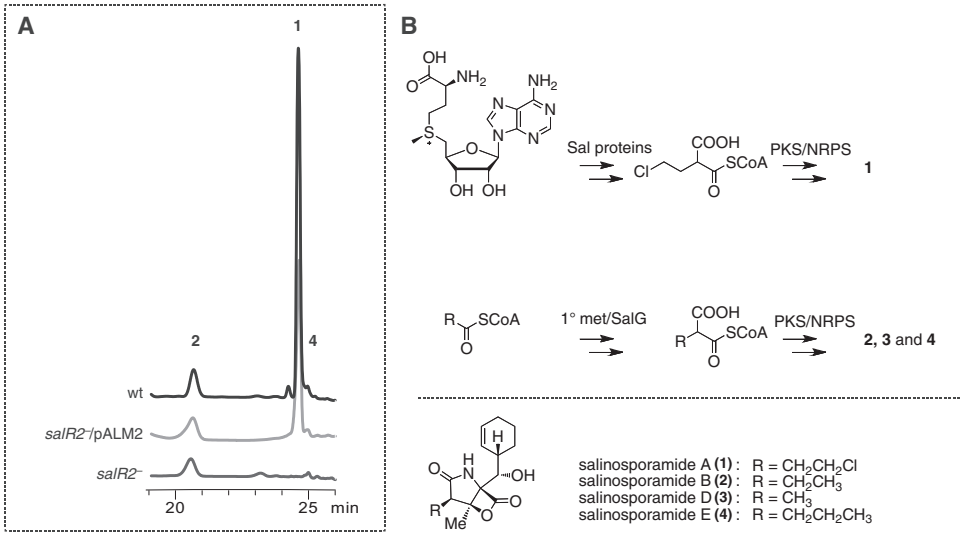

Figure 1. Gene Inactivation and Complementation of *salR2* in *S. tropica* CNB-440

(A) HPLC traces of *S. tropica* wild-type (wt) in black, *salR2*$^-$ mutant in gray, and in *trans* complemented mutant (*salR2*$^-$/pALM2) in light gray. Gene inactivation of *salR2* leads to selective reduction of salinosporamide A (**1**) production without effect on the deschloro analogs salinosporamide B (**2**) and E (**4**). Production of salinosporamide D was not detected in these studies.

(B) Conversion of *S*-adenosyl-L-methionine to the salinosporamide A-specific precursor chloroethylmalonyl-CoA requires eight proteins encoded within the *sal* gene cluster (top panel). Additionally the Sal PKS/NRPS machinery also incorporates common extender units, which are derived from primary metabolism (middle panel). This leads to a suite of analogs (bottom panel). See also Figure S1.

suggested that SalR1 is a MerR-type regulator commonly involved in antibiotic resistance (Brown et al., 2003), SalR2 is an unusual member of the LuxR-type subfamily of response regulators lacking a cognate histidine kinase (see Figure S1 available online) (Gao et al., 2007; Hutchings, 2007), and SalR3 is a putative LysR-type transcriptional regulator (Maddocks and Oyston, 2008). We interrogated the function of each regulatory gene through gene inactivation in which we replaced each gene with an apramycin-resistance cassette as previously described (Eustáquio et al., 2008; Gust et al., 2003). Metabolic profiling of the *salR1*$^-$ and *salR3*$^-$ deletion mutants did not show any significant effect on salinosporamide production. A duplicate *salR3* locus (strop_1049) also resides outside the *sal* biosynthetic gene cluster, where it may complement the function of *salR3* (strop_1032). Chemical analysis of the *salR2*$^-$ mutant, on the other hand, revealed a striking difference compared to the parental strain. Production of the chlorinated major compound salinosporamide A was nearly abolished to trace wild-type levels, whereas no effect was observed on the production of the deschloro analogs, salinosporamides B and E (Figure 1A). To further verify that gene inactivation of *salR2* alone was responsible for the observed phenotype, we applied genetic *in trans* complementation. The pSET152-based integration vector pALM2 was designed to express *salR2* under native promoter control. After vector integration, the new mutant *salR2*$^-$/pALM2 restored salinosporamide A biosynthesis (Figure 1A). The selective attenuation of salinosporamide A production strongly suggested that the SalR2 regulatory function is dedicated to chloroethylmalonyl-CoA biosynthesis (Figure 1B). Furthermore, gene inactivation of *salR2* did not cause any difference in growth compared to the parental strain (Figure 2A).

SalR2 Activates Early Steps in Chloroethylmalonyl-CoA Biosynthesis

Transcription of representative *sal* genes was investigated in the wild-type as well as the *salR2*$^-$ strain. To gain insight about the timing of *sal* gene expression, we examined the relation between growth and salinosporamide A production as well as transcription of representative genes in *S. tropica* CNB-440. Salinosporamide A production exhibited a growth-dependent pattern that was initiated in the late exponential phase and reached maximum yields during the transition phase around day 5 (Figure 2). Based on these data, two time points at which salinosporamides were being actively produced and *sal* genes actively transcribed (corresponding to days 2 and 3) were chosen as sample points for further transcriptional analysis. The comparative transcription profiles of *S. tropica* wild-type and the *salR2*$^-$ mutant at late exponential and early stationary phase are shown in Figure 3. All analyzed *sal* genes are transcribed in both strains, except for the two operons *salNO* and *salML*, which are transcribed from oppositely oriented promoters. Three of these gene products are known to be involved in chloroethylmalonyl-CoA biosynthesis (Eustáquio et al., 2009; Kale et al., 2010). The function of the fourth, the putative cyclase gene *salO* (27% identity to DpsY from *Streptomyces peucetius*), on the other hand, is unknown and may participate in the cyclization of the γ-lactam-β-lactone bicycle (Lomovskaya et al., 1998). To assess its involvement in salinosporamide biosynthesis, we inactivated it by PCR-targeted mutagenesis. The resulting mutant maintained wild-type production levels of all salinosporamides, which thereby suggests that SalO is not directly involved in salinosporamide biosynthesis as originally considered.

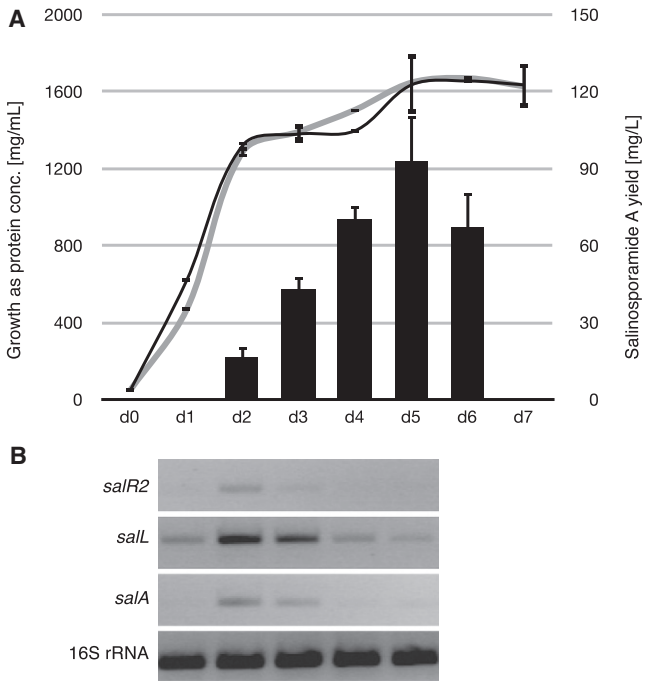

Figure 2. Growth-Dependent Salinosporamide A Biosynthesis

(A) Growth curve of *S. tropica* CNB-440 in black and *salR2*$^{-}$ mutant in gray on the primary axis (lines) in relation to salinosporamide A production on the secondary axis (columns). Each analysis was carried out in duplicate. Error bars represent the standard deviation.

(B) Reverse-transcription time course of the regulatory gene *salR2*, the chlorinase gene *salL* and the PKS gene *salA* as well as 16S rRNA control. Starting at day 1, samples were taken on five consecutive days from a *S. tropica* CNB-440 culture. Error bars represent the standard deviation.

Combined with the inactivation experiments, the transcriptional analysis results described previously suggest that SalR2 regulates the early steps in the biosynthesis of chloroethylmalonyl-CoA through transcriptional activation of *salL*, *salM*, and *salN,* but not of *salQ*, *salH*, *salG*, *salS* and *salT*. To provide a third line of evidence, we carried out a chemical complementation experiment in which the *salR2*$^{-}$ mutant was supplemented with the late intermediate analog 4-chlorocrotonic acid in order to restore salinosporamide A biosynthesis through action of the crotonyl-CoA reductase/carboxylase SalG (Eustáquio et al., 2009). Supplementation of the first pathway intermediate generated by chlorinase SalL, 5′-chloro-5′-deoxyadenosine (ClDA), was used as a negative control. Indeed, 4-chlorocrotonic acid restored salinosporamide A production in the *salR2*$^{-}$ mutant, whereas ClDA did not (Figure 4).

SalR2 Binds Specifically to the *salM-salN* and *salR2-salQ* Intergenic Regions

The gene product of *salR2* is a 24.3 kDa protein displaying two distinctive domains as identified by a Pfam search (Figure S1; Finn et al., 2010). The *N*-terminus contains an atypical receiver domain of response regulators (O'Connor and Nodwell, 2005; Ruiz et al., 2008; Schär et al., 2005; Tian et al., 2007; Wang et al., 2009), which is paired with a *C*-terminal LuxR-type DNA binding domain (Fuqua et al., 2001). Because transcription of the divergent operons *salNO* (phosphatase; conserved hypothetical) and *salML* (dehydrogenase; SAM-dependent chlorinase) was shown to directly depend on SalR2 activity, we hypothesized that SalR2 binds to the bidirectional *salM-salN* promoter region. Furthermore, LuxR-type proteins are known to bind to their own promoter in order to repress or stimulate transcription (Fuqua et al., 1994). To address the proposed functions, we carried out DNA binding studies (Figure 5) using electromobility shift assays (EMSA) with recombinant SalR2, which was produced as a *N*-terminal His_8-fusion protein from *Escherichia coli*. As DNA probes, we chose the full intergenic region between *salN* and *salM* ($P_{M\text{-}N}$), as well as a fragment located 60 to 320 nt upstream of the *salR2* translational start codon ($P_{R2\text{-}Q}$). As a negative control, we used a fragment isolated from the multiple cloning site of the vector pSET152 (NC). The recombinant SalR2 protein showed clear and specific binding to fragments $P_{M\text{-}N}$ and $P_{R2\text{-}Q}$ (Figures 5B and 5D).

To further identify specific SalR2 DNA binding sites, we carried out bioinformatics analysis based on the knowledge that LuxR-like regulators usually bind to a 20 bp inverted repeat similar to the *lux* box (Fuqua et al., 2001). We identified multiple 20-bp-long, imperfect inverted repeats in the *salM-salN* and the *salR2-salQ* intergenic regions (Figures 5A and 5E). The consensus sequence from the two sites of *salM-salN* contains six strictly conserved nucleotides separated by a 10-nt spacer: CTG-(N_{10})-CAG, whereas the sequence for the *salR2-salQ* site contains one mismatch, that is, CTG-(N_{10})-CAA. The consensus sequences are in agreement with the *lux* box of *Vibrio fischeri* in which at least five of the six bases are essential for LuxR binding (Antunes et al., 2008). To establish that this motif is essential for SalR2 binding, we altered the sequence of fragment $P_{M\text{-}N}$ by deleting the conserved residues CTG and CAG from both motifs. Indeed SalR2 was not able to bind to the mutated $P_{M\text{-}N}$ fragment as shown in Figure 5C.

To locate SalR2 binding sites relative to transcription start sites (*tss*), we employed the RACE ligation-mediated PCR approach (Tillett et al., 2000). Total RNA was extracted from mid-exponentially grown wild-type *S. tropica* and subjected to 5′-RACE as described in the Experimental Procedures. The detected RACE products for *salR2* and *salM* are shown in Figure S2A. The two *salR2* RACE products only differ 16 bp in size. Because the shorter cDNA fragment does not contain conserved motifs for sigma factor binding, it is thought to derive from a partially degraded mRNA product. Under the tested conditions, we therefore identified one transcription start site for *salR2* (*tss*-1), which is located 143 nt upstream of the translation start codon and is preceded by conserved sequences in the −35 (GCAGGC) and −10 (TAAAGT) regions (Figures S2B and S2C). Preliminary results from Roche 454 transcriptome sequencing revealed a second *salR2* transcription start site (*tss*-2) located 207 nt upstream of the *salR2* start codon and preceded by conserved sequences in the −35 (GCAGCA) and −10 (TAAGTT) regions (Figures S2B and S2C). The putative SalR2 binding site, which is identified as salR2-box3 in the *salR2-Q* intergenic region, is therefore centered at −33 relative to *tss-2*. To confidently assign the *salM tss*, we compared the initial 454 sequencing results with those obtained by RACE. The largest of the three *salM* RACE fragments contained conserved −10 and −35 motifs (Figures S2A and S2B), which was similarly found by 454 transcriptome sequencing. Based on

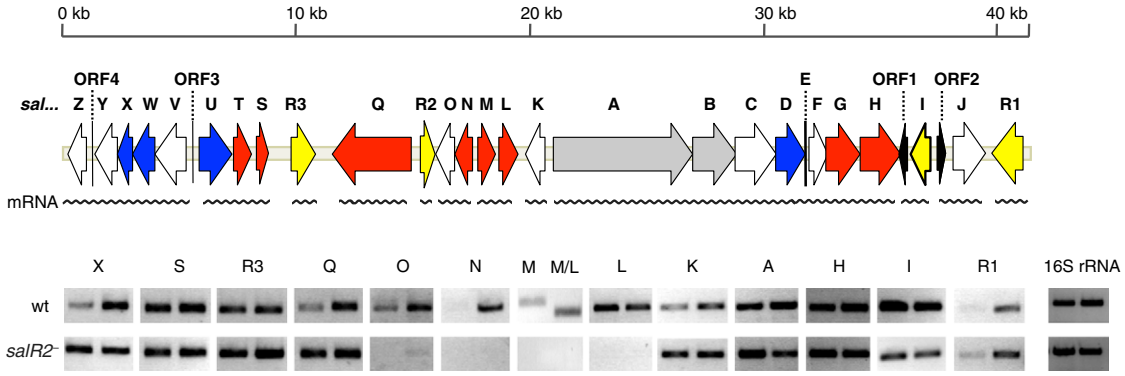

Figure 3. Semiquantitative Reverse-Transcription Analysis of *sal* Genes Comparing *S. tropica* CNB-440 (wt) and *salR2*⁻ Mutant

Total RNA was extracted from days 2 and 3, which were established as suitable data points (see Figure 2B). Putative transcription units (wavy lines) were predicted based on open reading frame organization and intergenic regions. In the *salM* panel we added the RT-PCR results of the *salM/L* intergenic region to prove co-transcription of *salM* and *salL*. Genes are color-coded based on confirmed/predicted function: assembly of core γ-lactam-β-lactone ring (gray), biosynthesis of chloroethylmalonyl-CoA (red) and of the nonproteinogenic amino acid L-3-cyclohex-2-enylalanine (blue), regulation and resistance (yellow), unknown (white), and two partial transposases (black).

these findings, the transcription start site was assigned at −81 relative to the translational start codon and to be preceded by sequences in the −35 (GCGGCG) and −10 (TAGCGT) regions (Figure S2D). The motif salR2-box2 is therefore centered at −64 relative to the *salM tss*. We were able to successfully identify transcription start sites for *salR2* and *salM*, but identification of a *salN* transcription start site remained unsuccessful using RACE. Furthermore, the sequencing coverage was insufficient for *salN* to confidently identify a *tss* using the 454 transcriptome results. Therefore, the function of the putative binding motif salR2-box1 remains unassigned at this point.

Overexpression of *salR2* Leads to Enhanced Salinosporamide A Production

Overexpression of pathway-specific activators has been reported to lead to increased production of various secondary

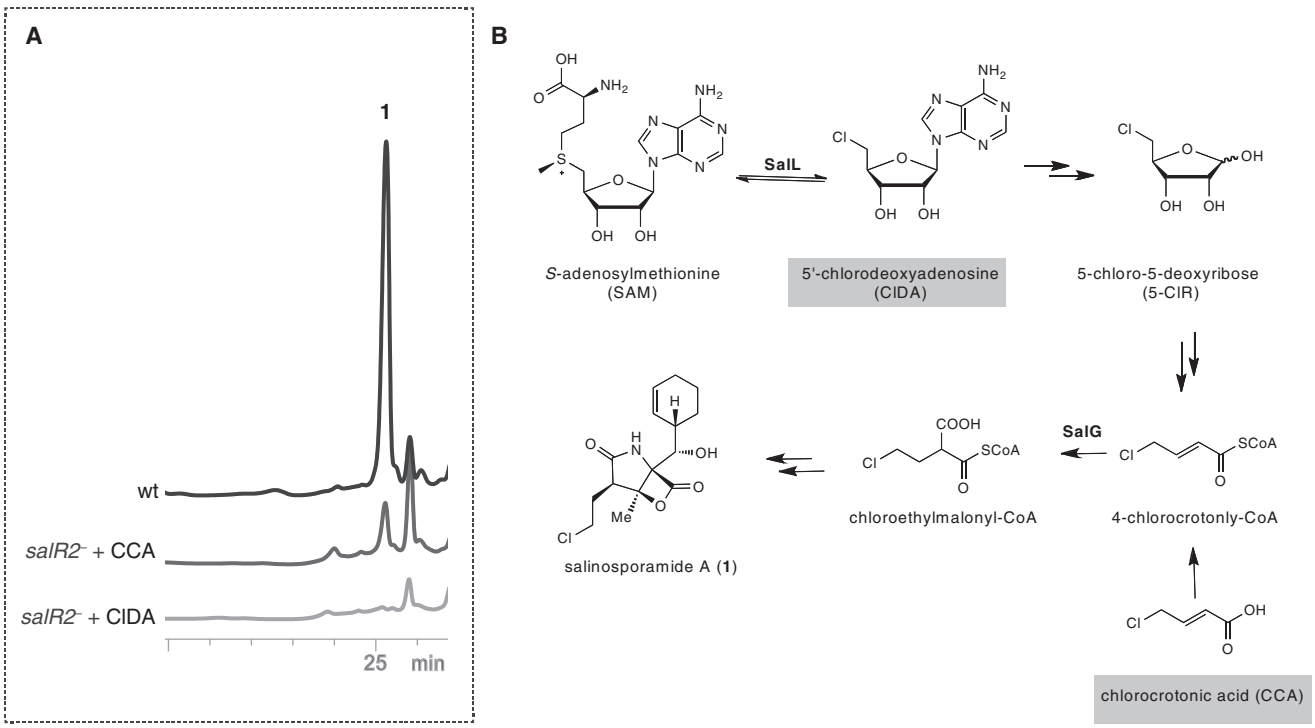

Figure 4. Chemical Complementation of the *salR2*⁻ Mutant

(A) HPLC traces of *S. tropica* wild-type (wt) in black, *salR2*⁻ mutant complemented with 4-chlorocrotonic acid (CCA) in gray and with 5′-chlorodeoxyadenosine (CIDA) in light gray.

(B) Biosynthetic scheme of the chloroethylmalonyl-CoA pathway showing two substrates used for chemical complementation (boxed).

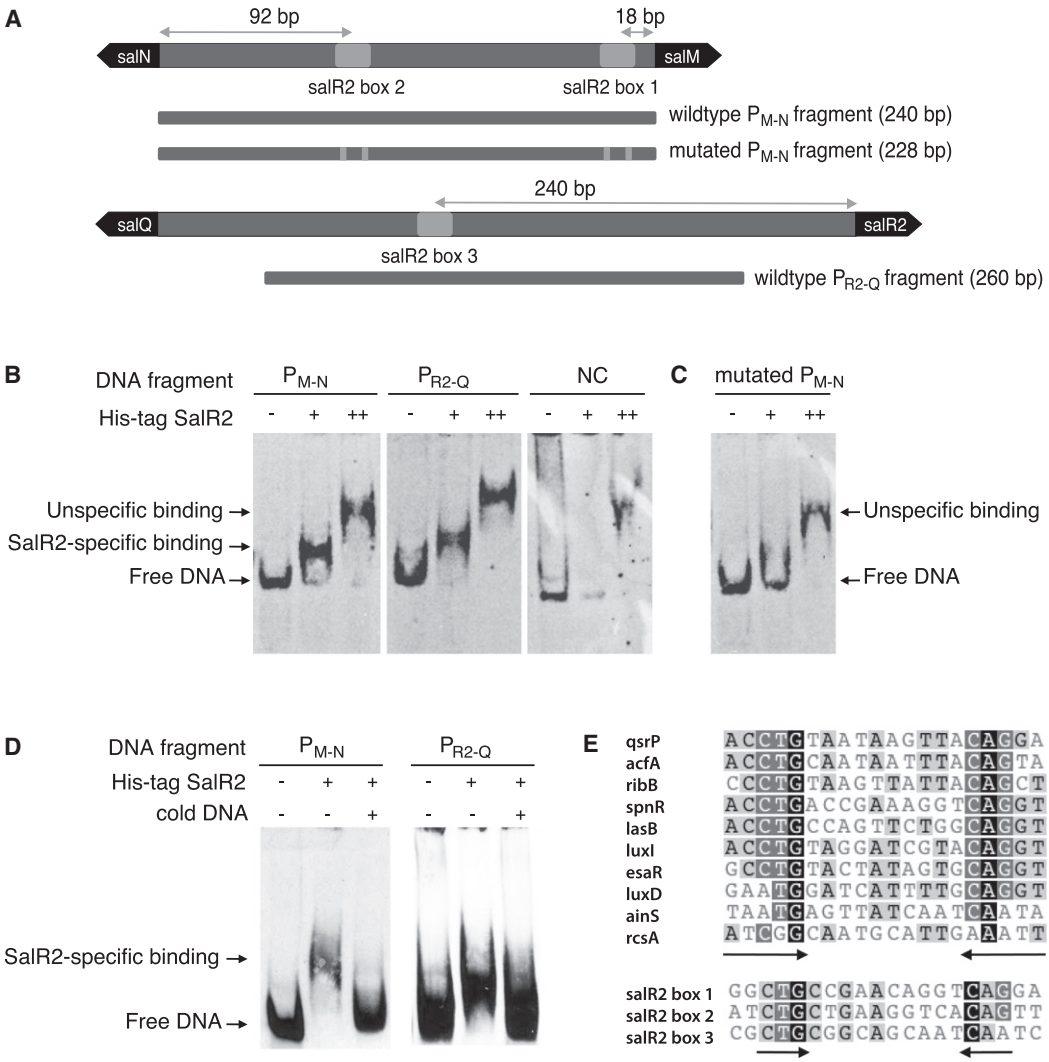

Figure 5. SalR2 DNA Binding Studies

(A) Schematic representation of *sal* DNA fragments used in the EMSA. Distances shown are relative to translational start codons and center of the putative SalR2 binding site.

(B) EMSA using 65 nM DNA (2 ng) and (–) no SalR2 protein or (+) and (++) increasing concentrations of purified, His_8-tagged SalR2, that is, 0.8 μM (0.4 μg) and 1.2 μM (0.6 μg), respectively. A fragment containing the multiple cloning site of pSET152 vector was used as negative control (NC). Note that high concentrations of SalR2 (++) lead to unspecific binding under the EMSA conditions tested as evidenced by binding to NC.

(C) EMSA using 65 nM of the mutated P_{M-N} DNA fragment and no protein (–) or 0.8 μM (+) and 1.2 μM (++) SalR2 protein. Deletion of the LuxR-type DNA binding motif present in the *salM-N* intergenic region abolishes SalR2 binding.

(D) Competition assay using 65 nM DNA and 0.8 μM His8-tagged SalR2. An additional 125-fold molar excess of specific competitor, nonlabeled DNA (cold DNA) was added when indicated (+).

(E) Alignment of known and putative LuxR-type binding motifs. Top panel represents alignment of verified lux boxes (Fuqua et al., 2001) located upstream of genes coding for QsrP (YP_207016), AcfA (YP_205361), RibB (YP_204085), LuxI (YP_206882), LuxD (YP_206880) and AinS (YP_204420) from *Vibrio fischeri* ES114, SpnR (AAN52499) from *Serratia marcescens*, LasB (AAZ81561) from *Pseudomonas aeruginosa,* EsaR (L32184) from *Pantoea stewartii* subsp. *stewartii* DC283 and RcsA (AY819768) from *Pantoea stewartii* subsp. *stewartii*. Bottom panel shows three putative SalR2 binding sites within the *sal* gene cluster, identified upstream of *salM*, *salN* and *salR2* respectively. See also Figure S2.

metabolites, which indicates a limiting role of the transcriptional activator in compound production (Liu et al., 2005; Lombó et al., 1999). We therefore intended to introduce additional *salR2* gene copies *in trans* in order to specifically increase salinosporamide A production. Earlier attempts in our laboratory to use the high copy vector pWHM3 (Vara et al., 1989) engineered to contain *ori*T for conjugative transfer in *Salinispora* remained unsuccessful. However, we knew from the previously mentioned complementation studies that the integrative vector pALM2 was suitable for genetic manipulations in *Salinispora*. The pSET152-based construct contains a ϕC31 *Streptomyces* phage-derived integrase gene and the phage attachment site *attP* (Thorpe et al., 2000). ϕC31 phage-based vectors have been widely used and shown to integrate in pseudo-*attB* sites (Combes et al., 2002).

We were able to identify three pseudo-integration sites in ten independent *S. tropica* mutant strains. pSET152-derived plasmids integrated in three open reading frames (*strop_0305, strop_0483,* and *strop_3569;* see Figure S3). Since pSET152 integration did not seem to have a negative effect on salinosporamide A production, we used pALM2 to introduce *salR2* into the wild-type strain. We also tested the activity of two candidate, vegetative promoters in the *S. tropica salR2* deletion mutant because no constitutive promoters were known for this genus. The first heterologous promoter tested was *ermE**p from *Saccharopolyspora erythraea* (Bibb et al., 1994). The construct pALM201—containing *salR2* under transcriptional control of *ermE**p—was, however, not able to restore salinosporamide A production in the *salR2*$^{-}$ mutant. We next tested the promoter of the apramycin resistance gene *aac(3)IV* because previous studies indicate high activity in the related *Actinoplanes friuliensis* (Wagner et al., 2009). The *aac(3)IV* promoter region, including its ribosome binding site, was isolated from pSET152 and cloned upstream of the *salR2* translation start codon to give pALMapra. This construct was able to restore salinosporamide A production in the *salR2*$^{-}$ mutant. We next introduced pALMapra into the wild-type strain and cultured two independent mutants in 24 deep-well plates (Siebenberg et al., 2010), allowing for more accurate salinosporamide quantification. Under these conditions, we observed a 2-fold selective increase of salinosporamide A for two independent wild-type/pALMapra mutants, whereas only a modest 1.3-fold increase for two wild-type/pALM2 mutants relative to the parental strain, and a negative control was achieved (Figure 6). We also compared the elevated salinosporamide A levels to production yields of salinosporamide B and E in the parental strain and two wild-type/pALMapra mutants. We found that salinosporamide A levels are increased 2-fold, whereas yields of the deschloro analogs remained at wild-type levels.

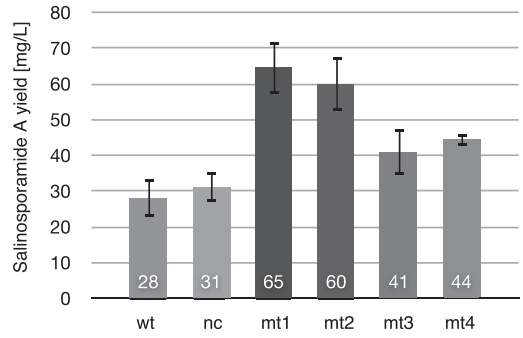

Figure 6. Overexpression of *salR2* under Control of a Constitutive Promoter (wt/pALMapra) and the Native Upstream Region (wt/pALM2)

Two independent wt/pALMapra mutants (mt1 and mt2) show 2-fold increase in salinosporamide A production compared to the wild-type (wt) and control strain wt/pALM0 (nc). In contrast, only a modest increase was observed in two independent wt/pALM2 mutants (mt3 and mt4). Average production levels are shown inside each graph bar. Error bars represent the standard deviation.

DISCUSSION

This study provides new insight into the regulated biosynthesis of chloroethylmalonyl-CoA, which is a specific precursor of the promising anticancer agent salinosporamide A. SalR2 chiefly controls the divergently transcribed *salNO* and *salML* gene pairs that include the unique biosynthetic enzyme SalL, which initiates the diversion of the important cofactor SAM from primary metabolism to this dedicated secondary metabolic pathway (Eustáquio et al., 2008).

Many of the secondary metabolic pathways explored to date involve regulators that control the expression of biosynthetic enzymes crucial for the synthesis of the core natural product skeleton (Martín and Liras, 2010) and therefore result in the general flux of pathway mixtures versus individual analogs. Secondary metabolic pathways naturally lead to compound mixtures and originate from a multitude of metabolic scenarios that include partial intermediate processing by tailoring enzymes, the inherent chemical reactivity of natural product intermediates, or in the case of the salinosporamides, the assembly of different precursor mixtures. Not only does building block supply contribute to product mixtures that result from substrate tolerant enzymatic processing, but supply is also a key contributor to metabolic flux and therefore production throughput. In the case of PKS-derived molecules, the supply of acyl-CoA starter and extender unit precursors has been shown to be one of the key rate-limiting steps in biosynthesis (Liu and Reynolds, 1999; Pulsawat et al., 2007). Increasing precursor supply, in other examples, has led to increased production yields, such as for the antitumor agent ansamitocin P-3 (Lin et al., 2011) and the antibiotic daptomycin (Huber et al., 1988). Orthogonal to these chemical complementation examples, the expression of precursor biosynthetic enzymes has been shown to be even more powerful in influencing production yields (Wang et al., 2011). The example described here with SalR2 represents another approach that involves the overexpression of a transcriptional activator of precursor biosynthesis genes.

LuxR-like proteins, such as SalR2, usually activate gene transcription by binding to *lux*-type boxes centered near position −42.5 (Devine et al., 1989) and less likely to promoter elements that are located further upstream. One example of the latter includes the activator binding site for UhpA from *E. coli* located at −64 from the *uhpT* tss (Merkel et al., 1992). This independent study is in agreement with SalR2's binding site at −64 from *salM*'s tss. Additionally, SalR2 was also shown to bind to a site (box3; Figure 5) at the −35 region of its own tss (*tss-2*). A likely conclusion is that SalR2 negatively autoregulates its own transcription, which is in agreement with previous reports on LuxR-type regulators (Cramer and Eikmanns, 2007).

The signal receiving domain of SalR2 holds an unusual response regulator sequence, which lacks a phosphorylation site (Figure S1). Other examples of atypical response regulators include JadR1 from *Streptomyces venezuelae* (Wang et al., 2009), NblR from *Synechococcus* sp. PCC 7942 (Ruiz et al., 2008), HP1021 and HP1043 from *Helicobacter pylori* (Schär et al., 2005), and RamR (O'Connor and Nodwell, 2005) and WhiI (Tian et al., 2007) from *Streptomyces coelicolor* A3(2). These examples, including SalR2, lack a cognate histidine kinase, and, therefore, a phosphorylation-independent mode of activation is likely necessary for SalR2 function.

Curiously, a SalR2 homolog (FIG, 34% identity) resides in the fluorometabolite biosynthesis cluster in *Streptomyces cattleya* (Huang et al., 2006). The *fl* locus shares homology with two structural genes of the *sal* gene locus—the fluorinase *flA* and the purine nucleotide phosphorylase *flB* are closely related to *salL* and *salT*, respectively. On the other hand, comparison of the related salinosporamide K and cinnabaramide biosynthetic loci in "*S. pacifica*" strain CNT-133 (Eustáquio et al., 2011) and *Streptomyces* sp. JS360 (Rachid et al., 2011), respectively, revealed that *salR2* and all eight chloroethylmalonyl-CoA pathway genes are absent. These observations suggest that the chloroethylmalonyl-CoA-specific regulator *salR2* was transferred to the *S. tropica sal* locus together with the genes that encode the chlorinated PKS building block, thereby resulting in its regulated assembly separate from that of the main salinosporamide molecule.

SIGNIFICANCE

Salinosporamide A is a clinically promising anticancer agent produced by *Salinispora tropica*. As salinosporamide A is presently being manufactured by saline fermentation for clinical trials (Potts et al., 2011), methods to increase yields are important in lowering the cost of production as this drug candidate moves beyond phase I clinical evaluation. A prerequisite to manipulate production of salinosporamide A is an extensive set of genetic tools. However, many expression plasmids and promoters (constitutive or inducible) developed for *Streptomyces* are not applicable for other actinomycetes. Therefore, this study allowed us to expand the genetic tool box for a very prolific but nonstreptomycete, marine-obligate genus. Using a multidisciplinary approach we showed that SalR2 is a pathway-specific regulator of chloroethylmalonyl-CoA biosynthesis that is a dedicated PKS substrate of salinosporamide A. This mode of regulation of a biosynthetic precursor in polyketide assembly is to the best of our knowledge unique. Furthermore, the ectopic overexpression of SalR2 under constitutive promoter control was key to our ability to selectively double the production yield of salinosporamide A without increasing the production levels of its minor analogs.

EXPERIMENTAL PROCEDURES

Bacterial Strains and Growth Conditions

Bacterial strains and plasmids used in this study are listed in Table S1. *Salinispora tropica* CNB-440 and its derivatives were routinely cultured in Erlenmeyer flasks containing a stainless steel spring and A1 sea water-based medium at 28°C (Beer and Moore, 2007). The REDIRECT technology kit for PCR targeting (Gust et al., 2003) was obtained from Plant Bioscience Limited (Norwich, UK). pCC1FOS-based (Epicenter) fosmid BHXS1782, which contains the *sal* gene cluster, except *salR1* and *salJ,* was used for gene replacement of *salR2* and *salR3*. Fosmid BHXS3930 was used instead for gene replacement of *salR1*. For selection of recombinant strains, the following antibiotics were used in indicated concentrations: apramycin (200 μg/ml for *S. tropica*; 50 μg/ml for *E. coli*), chloramphenicol (5 μg/ml for *S. tropica*; 12-25 μg/ml for *E. coli*), carbenicillin (100 μg/ml), kanamycin (50 μg/ml for *E. coli*), streptomycin (10 μg/ml for *S. tropica*; 50 μg/ml for *E. coli*), spectinomycin (50-100 μg/ml for *S. tropica*; 50 μg/ml for *E. coli*), and nalidixic acid (100 μg/ml). DNA isolation and manipulation were performed in accordance with standard procedures (Kieser et al., 2000; Sambrook and Russell, 2001). Derivatives of the *E. coli*/*Streptomyces* shuttle vector pSET152 (Bierman et al., 1992; Kuhstoss and Rao, 1991) were generated during this work (Table S1) and used to introduce *salR2* gene copies in *trans* into the *S. tropica* chromosome.

Growth Measurement in *Salinispora tropica*

Cell growth of *S. tropica* is difficult to measure by standard spectrometric methods, such as optical density, because this actinomycete forms cell aggregates. We therefore turned to a simple protein extraction protocol to measure cell growth over time. Cells were sampled and processed as described previously (Meyers et al., 1998). Ultra-violet (UV) absorptions at 230 nm and 260 nm were measured using a Nanodrop 1000, and total protein concentration was calculated using the equation: Total protein (mg/ml) = (183 x A_{230}) − (75.8 x A_{260}).

Purification of Recombinant SalR2

The gene *salR2* was amplified by PCR from fosmid BHXS1782 using the primer pair FP/RP-pAL4, cut with HindIII and XhoI, and ligated into the same sites of pHIS8 (Jez et al., 2000) yielding plasmid pHIS8-salR2, which was used to transform *E. coli* BL21(DE3)pLysS. The resulting transformant was inoculated in 3 l of auto-induction medium supplemented with 100 μg/ml of kanamycin (Studier, 2005) and grown at 28°C for 16–18 hr. Cells were harvested by centrifugation and frozen at –20°C. All purification steps were carried out at 4°C. Buffer B contained 50 mM NaH_2PO_4 (pH 8.0), 500 mM NaCl, 10% glycerol, and 10 mM 2-mercaptoethanol, as well as varying imidazole concentrations in mM range as indicated by the number of the buffer name. Frozen cells were thawed in 30 ml buffer B5 and 1% Tween. After the cell pellet was completely resuspended, lysozyme (1 mg/ml) was added and the mixture was incubated for 30 min with stirring. The suspension was sonicated for 3 min in 10 s on/off cycles. Cell debris were removed by centrifugation for 30 min at 20000 rpm. The cleared supernatant was mixed with 1 ml pre-equilibrated Ni-NTA agarose (Qiagen) and incubated for 60 min under gentle stirring. The protein-Ni-NTA slurry was collected by centrifugation (6000 rpm for 10 min), washed with 50 ml buffer B5 to separate from unbound protein, and resuspended in buffer B20. His_8-SalR2 was further purified on column by extensive washing with 20 ml buffer B20, 10 ml buffer B40, and 10 ml buffer B60 followed by an elution step with 2.5 ml buffer B250. In the final desalting and concentration steps, the protein was applied on a PD-10 column (GE healthcare), eluted in 3.5 ml storage buffer (50 mM NaH_2PO_4 (pH 7.9), 2 mM DTT), and concentrated 7-fold using a VIVASPIN 6 column (Sartorius) at 6000 rpm and 10°C. Aliquots of recombinant SalR2 protein were stored at −70°C until use in DNA-binding assays.

Gel Mobility Shift Assay

Gel shift assays were performed using the DIG Gel Shift Kit, 2nd Generation (Roche Molecular Biochemicals). The reaction was carried out at 25°C in 20 μl final volume containing 10 mM Tris/HCl (pH 7.5), 50 mM KCl, 1 mM DTT, 5 mM $MgCl_2$, 50 ng/μl poly [d (A-T)], 5 ng/uL poly L-lysine, 5% (w/v) glycerol, and approximately 0.4–0.6 μg of partially purified His_8-tagged SalR2. To identify specific binding, we added cold probe in 125-fold excess to the sample. After pre-incubation for approximately 5 min to establish an equilibrium, 2 ng DIG-labeled DNA fragment was added to each reaction and after an additional 15 min the mix was applied to a pre-run 5% (w/v) native polyacrylamide gel (BioRad) with 0.5x TBE as running buffer. The gel was run on ice at 55 V for 3–4 hr, transferred by electroblot to a positively charged Hybond-N^+ nylon membrane (Amersham Biosciences), and cross-linked under UV light for 3 min. Detection was carried out following the manufacturer's instructions and using the chemiluminescent substrate CSPD.

Inactivation of *sal* Genes and Genetic Complementation of *salR2*

Genes were inactivated using the PCR targeting system with some modifications as previously described (Eustáquio et al., 2008; Gust et al., 2003). For genetic complementation of the *S. tropica salR2*$^-$ mutant strain, we used a pSET152-based expression plasmid. See the Supplemental Experimental Procedures for details.

Construction of *salR2* Overexpression Plasmids under Control of Diverse Promoters

We constructed several pSET-derived integration vectors placing *salR2* under control of 1) its native promoter, 2) the constitutive *ermE** promoter from *Saccharopolyspora erythraea* (Bibb et al., 1985), and 3) the *aac(3)IV* promoter (Wagner et al., 2009), generating pALM2, pALM201, and pALMapra, respectively. See the Supplemental Experimental Procedures for details.

Isolation of Total RNA, cDNA Synthesis, and RT-PCR

S. tropica strains were grown in the same liquid medium as used for salinosporamide A production (see below). Aliquots (0.5–1 ml) were collected from a second-generation culture grown until late exponential and early stationary phase. Total RNA was extracted using the RiboPure-Bacteria kit (Ambion), and DNase I treatment was carried out for 5 hr following the manufacturer's instructions. Isolated RNA (50 ng) was tested by PCR for residual genomic DNA contamination using 16S rRNA as marker, then reverse-transcribed using the SuperScript III First-Strand Synthesis System for RT-PCR (Invitrogen). The resulting cDNA (50 ng/25 μl reaction), Taq polymerase (New England Biolabs), and RT-primers were used for RT-PCR under the following conditions: initial denaturation at 95°C for 2 min, 25–30 cycles of denaturation at 95°C for 30 s, annealing at 55°C for 30 s and extension at 72°C for 30 s, with a final extension step for 2 min. PCR primers for semiquantitative RT-PCR were designed for 13 putative transcription units based on their predicted operon structure, as well as the 16S rRNA gene as an internal control (Table S2). Oligonucleotides were designed using Primer3 software to generate fragments of about 250 bp in size.

Rapid Amplification of cDNA Ends

To identify transcription start sites for *salR2*, *salM,* and *salN*, we slightly modified the RACE protocol by Tillet et al. (Tillett et al., 2000). See the Supplemental Experimental Procedures for details.

Transcriptome Sequencing by 454

Total RNA from a second generation culture in late exponential phase was extracted using the RiboPure Bacteria kit (Ambion) and enriched for mRNA using MICROBExpress (Ambion), according to the manufacturer's instructions. After quality control (see the Supplemental Experimental Procedures), the mRNA-enriched sample was subjected to the GS FLX Titanium cDNA Rapid Library Preparation Method (Roche) and sequenced (one-half plate) using 454 technology. Mapper was run against the reference *S. tropica* genome (accession number NC_009380)—number of reads (557,992), number of bases (1.65 × 108), and average depth (0.7).

Chemical Complementation of Biosynthetic Intermediates

The two compounds 5′-chlorodeoxy-adenosine (5′-ClDA; Sigma Aldrich) and 4-chlorocrotonic acid (CCA; Eustáquio et al., 2009) were administered to the *S. tropica salR2*$^{-}$ mutant strain at a concentration of 0.33 mM after the first day of cultivation. Extraction and detection of salinosporamide A followed previous protocols (Eustáquio et al., 2009) as described below.

Analysis of Secondary Metabolites

For salinosporamide A production, *S. tropica* wild-type and mutant strains were cultivated using two different methods. The production medium for both cultivation methods was A1 sea water-based medium supplemented with 1% KBr, 0.4% Fe_2SO_4 and 0.1% $CaCO_3$. The standard fermentation was conducted in 250 ml Erlenmeyer flasks as described in the Supplemental Experimental Procedures. The production culture (50 ml) was started with 4% of a 3–4 day old (late exponential phase) pre-culture, and 2 g (dry weight) of XAD7 resin was added after 1 day of fermentation. The resin was extracted on day 5 with 25 ml acetone and processed as described below. For overexpression studies, we used 24-square deepwell plates (EnzyScreen BV, The Netherlands). Cultures were initially inoculated and grown in an Erlenmeyer flask for 24 hr as described previously (Siebenberg et al., 2010). After 1 day, 0.6% (w/v, final concentration) siloxylated ethylene oxide/propylene oxide copolymer Q2-5247 (Dow Corning, USA) was added to the cultures, and 3 ml aliquots were transferred to the 24-square deepwell plate containing 0.1 g sterile XAD7 resin. The resin was extracted with 3 ml acetone on day 6. All shakers used for Erlenmeyer flasks and deepwell plate cultivations were orbital shakers with 25 mm shaking diameter. The crude extract was dried and redissolved in 1 ml MeCN, then analyzed by HPLC with a Phenomenex C18 column (150 × 4.6 mm; 5 μm particle size) at flow rate of 1 ml/min, using isocratic 35% MeCN in water as the mobile phase with detection at 210 nm.

SUPPLEMENTAL INFORMATION

Supplemental information includes three figures and two tables and can be found with this article online at doi:10.1016/j.chembiol.2011.10.014.

ACKNOWLEDGMENTS

We kindly thank B. Gust and Plant Bioscience Limited for providing the REDIRECT© technology kit for PCR-targeting, A. Lapidus from the Joint Genome Institute for *sal* fosmids, and W. Fenical and P. R. Jensen for the *S. tropica* strain. Financial support was provided by the National Institutes of Health (CA127622) to B.S.M., the GeneChip Microarray Core (Veterans Medical Research Foundation) for providing preliminary 454 sequencing data, the Albert and Anneliese Konanz Foundation, Mannheim, for a graduate fellowship to A.L., the DAAD for a postdoctoral fellowship to T.A.M.G., and the Life Sciences Research Foundation via a Tularik postdoctoral fellowship to A.S.E.

Received: August 16, 2011
Revised: September 30, 2011
Accepted: October 11, 2011
Published online: December 22, 2011

REFERENCES

Antunes, L.C., Ferreira, R.B., Lostroh, C.P., and Greenberg, E.P. (2008). A mutational analysis defines *Vibrio fischeri* LuxR binding sites. J. Bacteriol. *190*, 4392–4397.

Beer, L.L., and Moore, B.S. (2007). Biosynthetic convergence of salinosporamides A and B in the marine actinomycete *Salinispora tropica*. Org. Lett. *9*, 845–848.

Bibb, M.J., Janssen, G.R., and Ward, J.M. (1985). Cloning and analysis of the promoter region of the erythromycin resistance gene (ermE) of *Streptomyces erythraeus*. Gene *38*, 215–226.

Bibb, M.J., White, J., Ward, J.M., and Janssen, G.R. (1994). The mRNA for the 23S rRNA methylase encoded by the ermE gene of *Saccharopolyspora erythraea* is translated in the absence of a conventional ribosome-binding site. Mol. Microbiol. *14*, 533–545.

Bierman, M., Logan, R., O'Brien, K., Seno, E.T., Nagaraja Rao, R., and Schoner, B.E. (1992). Plasmid cloning vectors for the conjugal transfer of DNA from Escherichia coli to Streptomyces spp. Gene *116*, 43–49.

Brown, N.L., Stoyanov, J.V., Kidd, S.P., and Hobman, J.L. (2003). The MerR family of transcriptional regulators. FEMS Microbiol. Rev. *27*, 145–163.

Combes, P., Till, R., Bee, S., and Smith, M.C. (2002). The streptomyces genome contains multiple pseudo-attB sites for the (phi)C31-encoded site-specific recombination system. J. Bacteriol. *184*, 5746–5752.

Cramer, A., and Eikmanns, B.J. (2007). RamA, the transcriptional regulator of acetate metabolism in *Corynebacterium glutamicum*, is subject to negative autoregulation. J. Mol. Microbiol. Biotechnol. *12*, 51–59.

Devine, J.H., Shadel, G.S., and Baldwin, T.O. (1989). Identification of the operator of the lux regulon from the *Vibrio fischeri* strain ATCC7744. Proc. Natl. Acad. Sci. USA *86*, 5688–5692.

Eustáquio, A.S., McGlinchey, R.P., Liu, Y., Hazzard, C., Beer, L.L., Florova, G., Alhamadsheh, M.M., Lechner, A., Kale, A.J., Kobayashi, Y., et al. (2009). Biosynthesis of the salinosporamide A polyketide synthase substrate chloroethylmalonyl-coenzyme A from S-adenosyl-L-methionine. Proc. Natl. Acad. Sci. USA *106*, 12295–12300.

Eustáquio, A.S., Nam, S.-J., Penn, K., Lechner, A., Wilson, M.C., Fenical, W., Jensen, P.R., and Moore, B.S. (2011). The discovery of salinosporamide K from the marine bacterium "*Salinispora pacifica*" by genome mining gives insight into pathway evolution. ChemBioChem *12*, 61–64.

Eustáquio, A.S., Pojer, F., Noel, J.P., and Moore, B.S. (2008). Discovery and characterization of a marine bacterial SAM-dependent chlorinase. Nat. Chem. Biol. *4*, 69–74.

Fenical, W., Jensen, P.R., Palladino, M.A., Lam, K.S., Lloyd, G.K., and Potts, B.C. (2009). Discovery and development of the anticancer agent salinosporamide A (NPI-0052). Bioorg. Med. Chem. *17*, 2175–2180.

Finn, R.D., Mistry, J., Tate, J., Coggill, P., Heger, A., Pollington, J.E., Gavin, O.L., Gunasekaran, P., Ceric, G., Forslund, K., et al. (2010). The Pfam protein families database. Nucleic Acids Res. *38* (Database issue), D211–D222.

Fuqua, W.C., Winans, S.C., and Greenberg, E.P. (1994). Quorum sensing in bacteria: the LuxR-LuxI family of cell density-responsive transcriptional regulators. J. Bacteriol. *176*, 269–275.

Fuqua, C., Parsek, M.R., and Greenberg, E.P. (2001). Regulation of gene expression by cell-to-cell communication: acyl-homoserine lactone quorum sensing. Annu. Rev. Genet. *35*, 439–468.

Gao, R., Mack, T.R., and Stock, A.M. (2007). Bacterial response regulators: versatile regulatory strategies from common domains. Trends Biochem. Sci. *32*, 225–234.

Groll, M., Huber, R., and Potts, B.C.M. (2006). Crystal structures of Salinosporamide A (NPI-0052) and B (NPI-0047) in complex with the 20S proteasome reveal important consequences of beta-lactone ring opening and a mechanism for irreversible binding. J. Am. Chem. Soc. *128*, 5136–5141.

Gulder, T.A.M., and Moore, B.S. (2010). Salinosporamide natural products: Potent 20S proteasome inhibitors as promising cancer chemotherapeutics. Angew. Chem. Int. Ed. Eng. *49*, 9346–9367.

Gust, B., Challis, G.L., Fowler, K., Kieser, T., and Chater, K.F. (2003). PCR-targeted *Streptomyces* gene replacement identifies a protein domain needed for biosynthesis of the sesquiterpene soil odor geosmin. Proc. Natl. Acad. Sci. USA *100*, 1541–1546.

Huang, F., Haydock, S.F., Spiteller, D., Mironenko, T., Li, T.L., O'Hagan, D., Leadlay, P.F., and Spencer, J.B. (2006). The gene cluster for fluorometabolite biosynthesis in *Streptomyces cattleya*: a thioesterase confers resistance to fluoroacetyl-coenzyme A. Chem. Biol. *13*, 475–484.

Huber, F.M., Pieper, R.L., and Tietz, A.J. (1988). The formation of daptomycin by supplying decanoic acid to *Streptomyces roseosporus* cultures producing the antibiotic complex A21978C. J. Biotechnol. *7*, 283–292.

Hutchings, M.I. (2007). Unusual Two Component Signal Transduction Pathways in the Actinobacteria. Advances in Applied Microbiology *61*, 1–26.

Jez, J.M., Ferrer, J.L., Bowman, M.E., Dixon, R.A., and Noel, J.P. (2000). Dissection of malonyl-coenzyme A decarboxylation from polyketide formation in the reaction mechanism of a plant polyketide synthase. Biochemistry *39*, 890–902.

Kale, A.J., McGlinchey, R.P., and Moore, B.S. (2010). Characterization of 5-chloro-5-deoxy-D-ribose 1-dehydrogenase in chloroethylmalonyl coenzyme A biosynthesis: substrate and reaction profiling. J. Biol. Chem. *285*, 33710–33717.

Kieser, T., Bibb, M.J., Buttner, M.J., Chater, K.F., and Hopwood, D.A. (2000). Practical *Streptomyces* Genetics (Norwich, United Kingdom: John Innes Foundation).

Kuhstoss, S., and Rao, R.N. (1991). Analysis of the integration function of the streptomycete bacteriophage φC31. J. Mol. Biol. *222*, 897–908.

Lin, J., Bai, L., Deng, Z., and Zhong, J.J. (2011). Enhanced production of ansamitocin P-3 by addition of isobutanol in fermentation of *Actinosynnema pretiosum*. Bioresour. Technol. *102*, 1863–1868.

Liu, H., and Reynolds, K.A. (1999). Role of crotonyl coenzyme A reductase in determining the ratio of polyketides monensin A and monensin B produced by *Streptomyces cinnamonensis*. J. Bacteriol. *181*, 6806–6813.

Liu, G., Tian, Y., Yang, H., and Tan, H. (2005). A pathway-specific transcriptional regulatory gene for nikkomycin biosynthesis in *Streptomyces ansochromogenes* that also influences colony development. Mol. Microbiol. *55*, 1855–1866.

Liu, Y., Hazzard, C., Eustáquio, A.S., Reynolds, K.A., and Moore, B.S. (2009). Biosynthesis of salinosporamides from alpha,beta-unsaturated fatty acids: implications for extending polyketide synthase diversity. J. Am. Chem. Soc. *131*, 10376–10377.

Lombó, F., Braña, A.F., Méndez, C., and Salas, J.A. (1999). The mithramycin gene cluster of *Streptomyces argillaceus* contains a positive regulatory gene and two repeated DNA sequences that are located at both ends of the cluster. J. Bacteriol. *181*, 642–647.

Lomovskaya, N., Doi-Katayama, Y., Filippini, S., Nastro, C., Fonstein, L., Gallo, M., Colombo, A.L., and Hutchinson, C.R. (1998). The *Streptomyces peucetius* dpsY and dnrX genes govern early and late steps of daunorubicin and doxorubicin biosynthesis. J. Bacteriol. *180*, 2379–2386.

Macherla, V.R., Mitchell, S.S., Manam, R.R., Reed, K.A., Chao, T.H., Nicholson, B., Deyanat-Yazdi, G., Mai, B., Jensen, P.R., Fenical, W.F., et al. (2005). Structure-activity relationship studies of salinosporamide A (NPI-0052), a novel marine derived proteasome inhibitor. J. Med. Chem. *48*, 3684–3687.

Maddocks, S.E., and Oyston, P.C.F. (2008). Structure and function of the LysR-type transcriptional regulator (LTTR) family proteins. Microbiology *154*, 3609–3623.

Martín, J.-F., and Liras, P. (2010). Engineering of regulatory cascades and networks controlling antibiotic biosynthesis in *Streptomyces*. Curr. Opin. Microbiol. *13*, 263–273.

Merkel, T.J., Nelson, D.M., Brauer, C.L., and Kadner, R.J. (1992). Promoter elements required for positive control of transcription of the *Escherichia coli uhpT* gene. J. Bacteriol. *174*, 2763–2770.

Meyers, P.R., Bourn, W.R., Steyn, L.M., van Helden, P.D., Beyers, A.D., and Brown, G.D. (1998). Novel method for rapid measurement of growth of mycobacteria in detergent-free media. J. Clin. Microbiol. *36*, 2752–2754.

O'Connor, T.J., and Nodwell, J.R. (2005). Pivotal roles for the receiver domain in the mechanism of action of the response regulator RamR of *Streptomyces coelicolor*. J. Mol. Biol. *351*, 1030–1047.

Potts, B.C., X Albitar, M., C Anderson, K., Baritaki, S., Berkers, C., Bonavida, B., Chandra, J., Chauhan, D., C Cusack, J., Jr., Fenical, W., et al. (2011). Marizomib, a proteasome inhibitor for all seasons: preclinical profile and a framework for clinical trials. Curr. Cancer Drug Targets *11*, 254–284.

Pulsawat, N., Kitani, S., Kinoshita, H., Lee, C.K., and Nihira, T. (2007). Identification of the bkdAB gene cluster, a plausible source of the starter-unit for virginiamycin M production in *Streptomyces virginiae*. Arch. Microbiol. *187*, 459–466.

Rachid, S., Huo, L., Herrmann, J., Stadler, M., Köpcke, B., Bitzer, J., and Müller, R. (2011). Mining the cinnabaramide biosynthetic pathway to generate novel proteasome inhibitors. ChemBioChem *12*, 922–931.

Ruiz, D., Salinas, P., Lopez-Redondo, M.L., Cayuela, M.L., Marina, A., and Contreras, A. (2008). Phosphorylation-independent activation of the atypical response regulator NblR. Microbiology *154*, 3002–3015.

Sambrook, J., and Russell, D. (2001). Molecular Cloning: A Laboratory Manual (Cold Spring Harbor, New York: Cold Spring Harbor).

Schär, J., Sickmann, A., and Beier, D. (2005). Phosphorylation-independent activity of atypical response regulators of *Helicobacter pylori*. J. Bacteriol. *187*, 3100–3109.

Siebenberg, S., Bapat, P.M., Lantz, A.E., Gust, B., and Heide, L. (2010). Reducing the variability of antibiotic production in Streptomyces by cultivation in 24-square deepwell plates. J. Biosci. Bioeng. *109*, 230–234.

Studier, F.W. (2005). Protein production by auto-induction in high density shaking cultures. Protein Expr. Purif. *41*, 207–234.

Thorpe, H.M., Wilson, S.E., and Smith, M.C. (2000). Control of directionality in the site-specific recombination system of the *Streptomyces phage* phiC31. Mol. Microbiol. *38*, 232–241.

Tian, Y., Fowler, K., Findlay, K., Tan, H., and Chater, K.F. (2007). An unusual response regulator influences sporulation at early and late stages in *Streptomyces coelicolor*. J. Bacteriol. *189*, 2873–2885.

Tillett, D., Burns, B.P., and Neilan, B.A. (2000). Optimized rapid amplification of cDNA ends (RACE) for mapping bacterial mRNA transcripts. Biotechniques *28*, 448, 450, 452–453, 456.

Vara, J., Lewandowska-Skarbek, M., Wang, Y.G., Donadio, S., and Hutchinson, C.R. (1989). Cloning of genes governing the deoxysugar portion of the erythromycin biosynthesis pathway in *Saccharopolyspora erythraea (Streptomyces erythreus)*. J. Bacteriol. *171*, 5872–5881.

Wagner, N., Osswald, C., Biener, R., and Schwartz, D. (2009). Comparative analysis of transcriptional activities of heterologous promoters in the rare actinomycete *Actinoplanes friuliensis*. J. Biotechnol. *142*, 200–204.

Wang, L., Tian, X., Wang, J., Yang, H., Fan, K., Xu, G., Yang, K., and Tan, H. (2009). Autoregulation of antibiotic biosynthesis by binding of the end product to an atypical response regulator. Proc. Natl. Acad. Sci. USA *106*, 8617–8622.

Wang, J.B., Pan, H.X., and Tang, G.L. (2011). Production of doramectin by rational engineering of the avermectin biosynthetic pathway. Bioorg. Med. Chem. Lett. *21*, 3320–3323.

